

Weakly attached cross-bridges in relaxed frog muscle fibers

D. W. G. Jung, T. Blangé, H. de Graaf, and B. W. Treijtel

Department of Physiology, University of Amsterdam, Amsterdam, The Netherlands

ABSTRACT Tension responses due to small, rapid length changes (completed within 40 μ s) were obtained from skinned single frog muscle fiber segments (4–10 mm length) incubated in relaxing and rigor solutions at various ionic strengths. The first 2 ms of these responses can be described with a linear model in which the fiber is regarded as a rod, composed of infinitely

small, identical segments, containing one undamped elastic element and two or three damped elastic elements and a mass in series. Rigor stiffness changed <10% in a limited range, 40–160 mM, of ionic strength conditions. Equatorial x-ray diffraction patterns show a similar finding for the filament spacing and intensity ratio I_{11}/I_{10} . Relaxed fibers became stiffer

under low ionic strength conditions. This stiffness increment can be correlated with a decreasing filament spacing and (an increased number of) weakly attached cross-bridges. Under low ionic strength conditions an additional recovery (1 ms time constant) became noticeable which might reflect characteristics of weakly attached cross-bridges.

INTRODUCTION

Recently, we described the similarities between tension responses of activated, relaxed and rigor skinned single frog muscle fibers to quick length changes completed within 40 μ s (Blangé et al., 1987; Jung et al., 1988b). We showed that the first 2 ms of these tension transients could be described with a model with either two relaxation times between three apparent elastic constants, in the case of rigor and relaxed fibers, or three relaxation times between four apparent elastic constants, in the case of activated fibers. The fast recovery of activated skinned fibers, which can be described with four apparent elastic constants, corresponds with the fast recovery of intact fibers (Ford et al., 1977). We concluded that all the elastic elements which were necessary to describe tension responses of activated and rigor fibers reflect to some extent cross-bridge numbers or properties. Furthermore, we showed equatorial x-ray reflections of activated, relaxed, and rigor single frog muscle fibers to support the conclusions drawn from the mechanical measurements. The results gave rise to questions about the number of cross-bridges in the activated and rigor state and the elastic properties of these cross-bridges. It was concluded that either the number of cross-bridges in rigor fibers equalled the number of cross-bridges in activated fibers, or the number of cross-bridges in the activated state was considerably less than in the rigor state. If this last possibility is true, and mass shift measurements obtained from equatorial x-ray diffraction patterns support this view, then nonlinear characteristics have to be assigned to rigor cross-bridges to explain the mechanical results.

Brenner et al. (1982, 1984) showed, by means of

stiffness measurements and equatorial x-ray diffraction patterns, that weakly attached cross-bridges are likely to be present in relaxed rabbit psoas muscle fibers, under low ionic strength conditions. These weakly attached cross-bridges could represent a step in the normal hydrolysis cycle, although this remains a point of discussion (Xu et al., 1987).

In this paper, we will describe the changes in stiffness which occurred when single frog muscle fibers were incubated in rigor and relaxing solutions under various conditions of ionic strength. Estimates will be made about the number of weakly attached cross-bridges in relaxed fibers at low ionic strength and the stiffness of these cross-bridges. The description of the tension transients, in response to fast length changes, in terms of model parameters (Jung et al., 1988b) is a suitable instrument to characterize these weakly attached cross-bridges in terms of elastic parameters. Results from equatorial x-ray diffraction measurements are given to support the mechanical evidence of weakly attached cross-bridges in relaxed muscle fibers of the frog at low ionic strength.

We will discuss some implications of our results in relation to the possibility of a certain amount of weakly attached cross-bridges in the activated state under normal ionic strength conditions. Preliminary results are described by Jung et al. (1987, 1988a).

METHODS AND MATERIALS

Preparation

All the mechanical and x-ray measurements were performed on single muscle fiber segments of the iliofibularis of the frog (*Rana esculenta*).

The method of preparing these freeze-dried fibers is described by Stienen and Blangé (1985) and Stienen et al. (1983). Freeze-dried fibers are suitable preparations to take accurate stiffness measurements with microsecond resolution, as has been shown previously (Blangé and Stienen, 1985a; Blangé and Stienen, 1985b; Jung et al., 1988b). Results from stiffness measurements of freeze-dried fibers are comparable with those obtained from fibers treated with Triton. Equatorial x-ray diffraction patterns of activated, rigor, and relaxed freeze-dried single fibers are comparable with those obtained from other preparation types (Jung et al., 1988b). In the experiments, fiber segments with a length ranging from 4 to 10 mm and a diameter ranging from 100 to 180 μm were used.

Solutions

A computer program was used to calculate the free concentrations of some important ions, pH, ionic strength and the amount of KOH/HCl and KCl necessary to adjust pH and ionic strength of the solutions to the values desired at a chosen solution temperature. The program is based on that of Fabiato and Fabiato (1979). Several stability constants mentioned by Godt and Lindley (1982) are used. Three types of solutions are used in this study: relaxing, activating, and rigor solution. In Table 1, the composition of these solutions, under control conditions (pH 7.00, temperature 4.0°C, ionic strength 160 mM) and under various ionic strength conditions are given. Relaxing solutions with a high MgATP concentration did not give different mechanical or x-ray diffraction results than relaxing solutions with a low MgATP concentration. In some experiments the relaxed fiber was compressed through the addition of various concentrations of Dextran (mol wt 200,000–275,000; BDH Chemicals Ltd., Poole, UK) to the relaxing solution under control conditions. In all solutions pH was set to 7.00 (± 0.05). The temperature of the solutions was kept at 4.0 (± 0.5)°C.

Mechanical measurements

Apparatus

The advanced displacement generator described by van den Hooff et al. (1982) enabled us to perform small and rapid length changes which

were completed within 40 μs . The force transducer, which (like the other devices uses) is described by Stienen and Blangé (1985), had a natural frequency in air of 55 kHz (50–55 kHz with the fiber mounted and placed in the solution), a sensitivity of 4.1 mV/mN with 5 μN noise and a damping time constant of 150 μs . We used a digital oscilloscope to record the tension transients and length changes with a sampling frequency of 500 and 2,000 kHz.

Model

The measured tension transients were simulated with a model based on a formalism described by Blangé and Stienen (1985b). Using this model, we assumed that a single muscle fiber segment could be regarded as a uniform rod, with circular cross-section, composed of small identical units which were connected in series with a density of 1,060 kg/m³. Each unit contains one undamped and two damped elastic elements (five-parameter model) or one undamped and three damped elastic elements in series (seven-parameter model) (see Fig. 1 A). The model simulations enabled us (Jung et al., 1988b) to describe the first 2 ms of tension transients in terms of parameters which are dependent on the specific configuration of the model elements (E_1 , E_2 , E_3 , μ_2 , μ_3 and if necessary E_4 and μ_4) and in terms of parameters which are independent on the configuration of the model elements (E_{app1} , E_{app2} , E_{app3} , τ_1 , τ_2 , and if necessary E_{app4} and τ_3). See Fig. 1 B. The apparent elastic constants are defined by:

$$\begin{aligned} E_{app1} &= E_1 \\ (E_{app2})^{-1} &= (E_{app1})^{-1} + (E_2)^{-1} \\ (E_{app3})^{-1} &= (E_{app2})^{-1} + (E_3)^{-1} \\ (E_{app4})^{-1} &= (E_{app3})^{-1} + (E_4)^{-1} \end{aligned}$$

Experimental protocol

The mounting procedure of the freeze-dried fibers as well as the method of measuring and modeling tension transients of these fiber segments are extensively described by Jung et al. (1988b). We used the following

TABLE 1 Composition of incubation solutions

Ionic	Imidazol	EGTA	EDTA	CP	MgATP	Free Ca ²⁺	Free Mg ²⁺	Free Na ⁺	Free K ⁺	Free Cl ⁻
Strength relaxing solutions										
30 (A)	10	2	—	—	2	0	1	4	11	16
30 (B)	10	0.5	—	—	4	0	1	8	5	13
50 (A)	10	2	—	—	2	0	1	4	31	36
50 (B)	10	0.5	—	—	5	0	1	11	22	30
100	60	15	—	10	5	0	1	31	23	40
160	60	20	—	10	5	0	1	31	45	51
220	60	20	—	10	5	0	1	51	85	111
280	60	20	—	10	5	0	1	51	144	171
Rigor solutions										
20	10	0.2	0.3	—	—	0	0	1	11	18
40	10	0.2	0.3	—	—	0	0	11	21	38
100	40	11	1	—	—	0	0	22	34	61
160	60	20	5	—	—	0	0	30	52	72
220	60	20	5	—	—	0	0	50	92	132
Activating solutions										
160	60	20	—	10	5	0.1	1	31	46	53

All concentrations given in millimoles. Relaxing and activating solutions contain 50 U/ml CK (creatine kinase). CP, creatine phosphate. Relaxing solutions 30(B) and 50(B) can be denoted as high-MgATP relaxing solutions. pH 7.00 at 4.0°C.

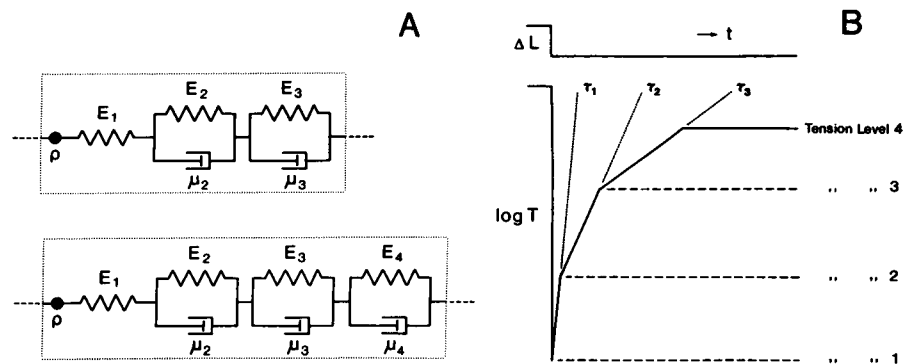


FIGURE 1 (A) The two mechanical equivalents of the half sarcomere used to simulate the first 2 ms of tension transients of activated, relaxed, and rigor fibers. The models will be denoted as "five-parameter model" and "seven-parameter model." E_1 represents an undamped elastic element, (E_2, μ_2), (E_3, μ_3), and (E_4, μ_4) represent damped elastic elements. The model parameters $E_1, E_2, E_3, \mu_2, \mu_3$ (and if necessary E_4 and μ_4) can be converted into a parameter representation, with apparent elastic constants and time constants, which is independent of the specific configuration of the model elements. (B) Schematic illustration of the parameter representation which is independent of the specific configuration of the model elements. The density component of the model is neglected and the length change is instantaneous. This parameter representation of tension transients consists of three (four) apparent elastic constants ($E_{app1}, E_{app2}, E_{app3}$, and if necessary E_{app4}), with corresponding tension levels, and two (three) time constants (τ_1, τ_2 , and if necessary τ_3) which represent the relaxation times between these levels.

procedure: after incubation in relaxing solution (ionic strength 160 mM) sarcomere length was adjusted to 2.15 μm under laser diffraction control. Tension transients of fibers incubated in activating, relaxing, and rigor solutions (ionic strength 160 mM), which we regarded as control measurements, were obtained several times during the experiment. The standard procedure in the control experiments consisted of incubation in 160 mM relaxing solution (at least 5 min) with recording of tension responses to length changes, 160 mM low-EGTA relaxing solution, 160 mM activation solution (at least 1 min) with recording of tension responses to length changes after development of a steady tension level, 160 mM relaxing solution (at least 5 min) with recording of tension responses to length changes, 160 mM rigor solution (5 min) with recording of tension responses to length changes after development of a steady tension level. The low-EGTA solution was similar to the relaxing solution, except that 20 mM EGTA was replaced by 0.2 mM EGTA and 19.8 mM HDTA (Moiescu and Thieleczek, 1978).

The standard procedure in the ionic strength experiments consisted of incubation in 160 mM relaxing solution (at least 5 min), relaxing solution of n mM ionic strength (at least 5 min) with recording of tension responses to length changes, rigor solution of n mM ionic strength (5 min) with recording of tension responses to length changes after development of a steady tension level, relaxing solution 160 mM. The order of changing the salt concentration of the incubation solution did not follow any fixed routine. However, tension transients obtained from fibers incubated in rigor solutions of high (220 mM) or low (20 mM) salt concentration were in general measured at the end of an experiment. These solutions caused, in some fibers, some loss of isometric tension of the activated and rigor fiber under control conditions. This pointed to irreversible changes in these fibers.

During each incubation, several tension transients (at least four), in response to rapid length changes with changing amplitude, were recorded. The amplitude of the length changes varied between 1.0 nm/half sarcomere shortening of the fiber and 3.0 nm/half sarcomere lengthening of the fiber. Each of these tension transients was analyzed in terms of model parameters. The interpolated parameter values at a length change of zero amplitude, obtained from the regression line, were used as a parameter estimate of the fiber in a given incubation solution. This procedure is, in relation to the parameter estimates of rigor,

relaxed, and activated fibers at control conditions, described by Jung et al. (1988b).

Several times during the experiment, the sarcomere length was checked in the relaxing solution by means of the laser diffraction pattern. Fiber diameter and fiber length were measured by means of a surgical microscope (accuracy 5%). During incubation in the solutions used, no differences in fiber diameter have been detected. Experiments were not continued when the steady isometric tension of a fully activated fiber in the control measurements at the end of the experiment had decreased >10%.

In the case of experiments with relaxed fibers compressed with Dextran a similar procedure, as described, was followed.

X-Ray measurements

Apparatus

Equatorial x-ray diffraction patterns of activated, relaxed, and rigor single fiber segments at various ionic strengths of the incubation solutions were obtained by the use of the small angle scattering facility (beamline 8.2) of the Synchrotron Radiation Source at Daresbury, UK. The distance between sample and the linear position sensitive detector was 2.00 m. Dimensions of the x-ray beam at the position of the sample were 4.0 mm (horizontal) and 0.4 mm (vertical). Wavelength of the x-ray beam was 0.148 nm. Muscle fibers were mounted between a glass rod and a force transducer. Incubation of the fibers took place in small cells which were temperature controlled. X-Ray diffraction patterns were recorded in small, temperature-controlled cells with mica windows. Typical sampling times were 10–20 s.

Model

The complete pattern on one side of the central beam was analyzed with a least squares fitting routine. No smoothing or averaging methods were used. The expression for the line shape of the diffraction pattern, which is used in the fitting procedure, is described by Jung et al. (1988b).

Masses associated with the actin and myosin filament were calculated from the Fourier projections. The calculations were made with the use of

amplitudes of the 10 and 11 reflections. The relative amount of material in actin and myosin filament expressed as a ratio A/M was calculated for two possible positions of the background. These values of A/M will be denoted as A/M (high), background level on the lowest electron density value in the whole Fourier projection, and A/M (low), background level on the lowest electron density value along the line that joins the actin and myosin filaments (Haselgrove and Huxley, 1973).

Experimental protocol

The mounting procedure is comparable with the one used in the mechanical experiments. We used the following procedure. After incubation in relaxing solution (160 mM ionic strength) sarcomere length was adjusted to $2.15\ \mu\text{m}$ under laser diffraction control. X-Ray diffraction patterns obtained from activated, relaxed, and rigor fibers (ionic strength 160 mM) were regarded as control diffraction patterns. These control measurements were not only performed at the beginning and end of each experiment, but also during the experiment. Consequently, three or four diffraction patterns, obtained from the fiber incubated in solutions with varying salt concentration, were sandwiched between control measurements. The standard procedure of incubation was the same as described in the experimental protocol of the mechanical measurements. During the experiment, at least 20 patterns were obtained from one fiber. No fixed sequence of incubating the fiber in rigor and relaxing solutions of varying salt concentration was followed, although extreme values of ionic strength (20 and 220 mM) were used at the end of an experiment. The sequence of the incubation had no influence on the results.

Equatorial diffraction patterns which were obtained from relaxed fibers compressed with Dextran were always sandwiched between control measurements.

The tension exerted by the fiber was continuously monitored during the experiment. Sarcomere length was inspected after each pattern that was obtained from an activated fiber. After the experiment, the fiber was inspected by means of a surgical microscope. We did not continue the experiment when the isometric tension of fully activated fibers decreased $>20\%$, or when the laser diffraction pattern became irregular. We confined ourselves to the analyses of experiments in which the x-ray diffraction patterns of the control measurements at the start and end of the experiment did not change $>10\%$ with respect to the intensity ratio I_{11}/I_{10} , or 2% with respect to d_{10} .

In the experiments described, no radiation damage of the fiber was observed. Irreversible microscopic structural changes in the central region of the illuminated fiber segment were only observed during an experiment in which the accumulated dose was three times that of the described measurements. The laser diffraction pattern of this damaged region of the fiber was irregular too. In this case, we also noticed a significant decrease of the isometric tension that was exerted by the fiber. All these effects did not appear in the experiments described.

RESULTS

Mechanical measurements

As described previously by Jung et al. (1988b), we were able to simulate the first 2 ms of tension responses of activated, relaxed, and rigor fibers, under control conditions (temperature 4.0°C , pH 7.0, ionic strength 160 mM) with the models shown in Fig. 1 A. For the description of the tension responses following a fast length change completed within $40\ \mu\text{s}$, we used either parameters which are dependent on the specific configuration of

the model elements (E_x and μ_x) or parameters which are independent on the configuration of the model elements (E_{appx} and τ_x). The model independent parameter representation is schematically illustrated in Fig. 1 B.

Relaxed fibers

Typical measured and simulated tension responses of relaxed fibers in various ionic strength solutions are shown in Fig. 2 A. General features of the first $500\ \mu\text{s}$ of the tension responses of relaxed fibers, as well as rigor fibers, after a fast length change are: a delay, an abrupt tension change, an oscillation, and a fast recovery. The measured delay is the time between the onset of the displacement and the tension change and thus corresponds to the initial transmission velocity of the disturbance in the fiber. The time course of the oscillation in the tension response points to a different transmission velocity. Evaluation of the tension responses by the simulation procedure reveals that this difference in transmission velocity is associated with a very fast relaxation time (within microseconds). The fast recovery corresponds with another fast relaxation time. The tension transients of relaxed fibers at 30, 50, and 100 mM ionic strength

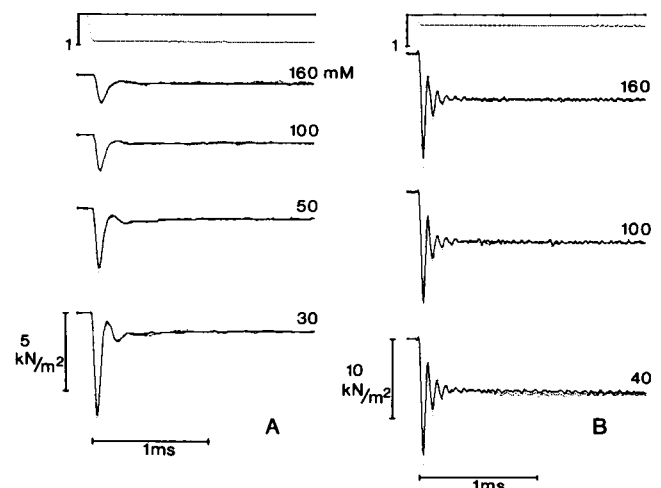


FIGURE 2 Typical measured and simulated tension responses of a fiber incubated in (A) relaxing solutions with various salt concentrations and (B) rigor solutions with various salt concentrations. (Upper traces) Displacement (lengthening of the fiber) expressed in nanometers per half sarcomere. (Lower traces) Tension responses (dotted curves) and simulations (solid curves). The small upward deflection at the beginning of each displacement and tension trace is due to digital filtering. All tension traces of relaxed fibers, except the one obtained in 160 mM ionic strength solution, were simulated with the seven-parameter model shown in Fig. 1 A. The tension transients of rigor fibers and high-ionic-strength relaxed fibers (160–280 mM) were simulated with the five-parameter model shown in Fig. 1 A. Conditions: sarcomere length $2.15\ \mu\text{m}$, pH 7.00, temperature 4.0°C , fiber length $5.6\ \text{mm}$, fiber diameter $180\ \mu\text{m}$, experiment 7 November 1986.

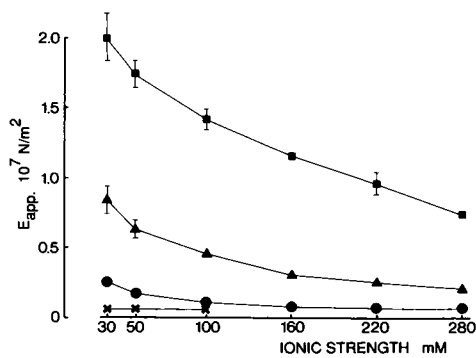


FIGURE 3 The four apparent elastic constants necessary to describe the first 2 ms of relaxed tension responses as function of the ionic strength of the incubation solution. E_{app1} (squares); E_{app2} (triangles); E_{app3} (circles), and E_{app4} (crosses). E_{app4} could not be resolved from tension responses obtained in solutions with a higher ionic strength than 100 mM. Data obtained from six fibers. Conditions: sarcomere length 2.15 μm , pH 7.0, temperature 4.0°C.

were simulated with the seven-parameter model because simulations with the five-parameter model resulted in unsatisfactory fits after 1 ms. Tension responses obtained from fibers incubated in the other relaxing solutions were simulated with the five-parameter model. The increased stiffness under low ionic strength conditions is expressed as a decreased delay between the start of the displacement

and the start of the tension response, an increased initial tension change, a decreased oscillation period and, in the case of stretches, an increased tension level after 500 μs (see Fig. 2 A). The effect of changing the ionic strength of the incubation solution on the stiffness of relaxed fibers is shown in Fig. 3. The first three apparent elastic constants (E_{app1} , E_{app2} , and E_{app3}) increase significantly with decreasing ionic strength. It furthermore illustrates that, under low ionic strength conditions, an additional recovery towards a fourth apparent elastic constant (E_{app4}) becomes noticeable. This recovery component, which might be present under higher ionic strength conditions, was too small to be resolved from the responses at high ionic strength. The time constants, associated with the recovery between the apparent elastic constants, as well as the specific model parameters are given in Table 2. The first two time constants (4 and 70 μs) do not depend on the ionic strength of the incubation solution. The value of the third time constant, which appeared to be present only under low ionic strength conditions, was close to 1 ms.

The normalized values of the specific model parameters of relaxed fibers are given in Fig. 4. The parameters E_1 and μ_2 increase to 175% at 30 mM compared with the values at 160 mM ionic strength. The increase of the values of the other parameters (E_2 , E_3 , and μ_3) is far more evident, up to 350% of the values obtained under control conditions. The increment of these parameters is, just as

TABLE 2 Model parameters and time constants of single frog muscle fibers as a function of ionic strength

Relaxed state Ionic strength	30	50	100	160	220	280	
E_1	2.00 ± 0.17	1.73 ± 0.10	1.42 ± 0.07	1.16 ± 0.03	0.95 ± 0.08	0.73 ± 0.01	$\cdot 10^7$
E_2	1.47 ± 0.20	1.02 ± 0.12	0.70 ± 0.08	0.43 ± 0.02	0.33 ± 0.01	0.31 ± 0.03	$\cdot 10^7$
E_3	0.37 ± 0.05	0.26 ± 0.04	0.15 ± 0.01	0.11 ± 0.01	0.10 ± 0.01	0.09 ± 0.01	$\cdot 10^7$
E_4	0.08 ± 0.01	0.10 ± 0.01	0.11 ± 0.01	—	—	—	$\cdot 10^7$
μ_2	1.40 ± 0.13	1.15 ± 0.11	1.06 ± 0.12	0.81 ± 0.06	0.64 ± 0.05	0.53 ± 0.04	$\cdot 10^2$
μ_3	6.83 ± 0.99	1.82 ± 0.64	3.12 ± 0.28	2.50 ± 0.36	2.10 ± 0.21	1.82 ± 0.24	$\cdot 10^2$
τ_1	3.8 ± 0.3	3.7 ± 0.2	4.3 ± 0.3	4.2 ± 0.3	4.4 ± 0.6	4.5 ± 0.4	
τ_2	6.5 ± 1.0	6.0 ± 0.6	5.9 ± 0.4	6.9 ± 0.7	7.3 ± 0.8	7.5 ± 1.3	$\cdot 10$
τ_3	1.1 ± 0.2	1.0 ± 0.3	0.9 ± 0.3	—	—	—	
Rigor state Ionic strength	20	40	100	160	220		
E_1	4.2 ± 0.1	4.7 ± 0.1	5.2 ± 0.2	4.8 ± 0.1	4.2 ± 0.2	$\cdot 10^7$	
E_2	5.1 ± 0.1	5.7 ± 0.3	5.2 ± 0.5	4.4 ± 0.3	3.2 ± 0.2	$\cdot 10^7$	
E_3	5.9 ± 0.5	5.4 ± 0.5	5.7 ± 0.7	4.8 ± 0.6	3.6 ± 0.2	$\cdot 10^7$	
μ_2	3.8 ± 0.1	3.8 ± 0.5	3.8 ± 0.5	3.3 ± 0.4	2.9 ± 0.3	$\cdot 10^2$	
μ_3	9.4 ± 4.9	6.9 ± 1.8	6.4 ± 1.4	6.1 ± 1.4	6.2 ± 1.0	$\cdot 10^3$	
τ_1	4.0 ± 0.1	3.6 ± 0.4	3.6 ± 0.4	3.4 ± 0.4	3.9 ± 0.4		
τ_2	11.2 ± 3.0	8.6 ± 1.7	7.5 ± 1.1	8.3 ± 1.1	11.9 ± 1.7	$\cdot 10$	

Parameter values of the model elements of relaxed and rigor fibers as a function of ionic strength and the time constants (which represent the recovery time between the apparent elastic constants) of relaxed and rigor fibers as a function of ionic strength. Ionic strength given in millimoles. Mean and standard error of the mean of E_1 , E_2 , E_4 are given in N/m^2 , μ_2 and μ_3 in Ns/m^2 . Mean and SEM of τ_1 and τ_2 were given in μs , τ_3 in ms. Data obtained from six fibers. Conditions as in Fig. 4.

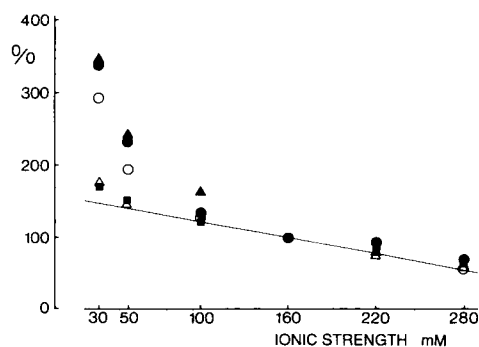


FIGURE 4 Normalized values of the first five (out of seven) model parameters of relaxed fibers as a function of ionic strength of the incubation solution. E_1 (solid squares), E_2 (solid triangles), μ_2 (open triangles), E_3 (solid circles), and μ_3 (open circles). All parameter values were normalized to the values obtained under the control conditions (160 mM). Conditions as in Fig. 3.

E_1 and μ_2 , rather small in the range of 280–100 mM and far more evident in the range of 100–30 mM.

Rigor fibers

Typical measured and simulated tension responses of rigor fibers in various ionic strength solutions are shown in Fig. 2 B. All tension transients were simulated with the five-parameter model. Under all ionic strength conditions tension responses of the rigor fibers were similar. The small effect on the stiffness of rigor fibers due to changes in the ionic strength of the solution is illustrated in Fig. 5. The three apparent elastic constants (E_{app1} , E_{app2} , and E_{app3}), which are necessary to describe the tension transients of rigor fibers satisfactorily, differ slightly (<10%) within the range of 40 to 160 mM ionic strength. At 220 mM all three apparent elastic constants tend to deviate

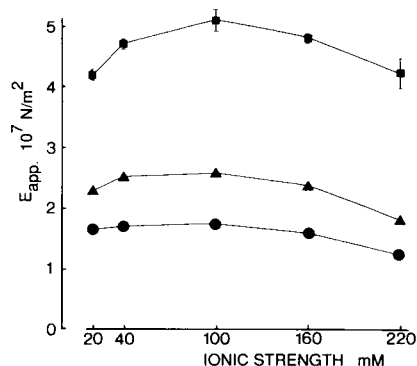


FIGURE 5 The three apparent elastic constants necessary to describe the first 2 ms of rigor tension responses as a function of the ionic strength of the incubation solution. E_{app1} (squares), E_{app2} (triangles), and E_{app3} (circles). Data obtained from six fibers. Conditions: sarcomere length 2.15 μm , pH 7.0, temperature 4.0°C.

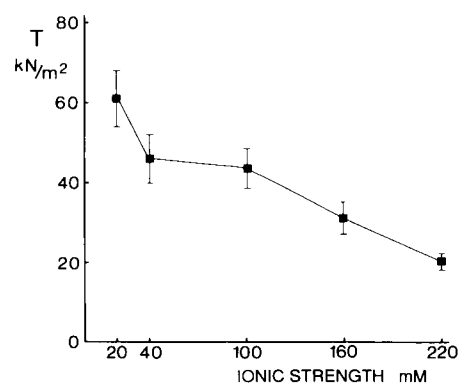


FIGURE 6 Isometric rigor tension at various ionic strengths of the incubation solutions. Data obtained from six fibers. Conditions as in Fig. 5.

>10% from the values obtained at 160 mM, whereas at 20 mM only E_{app1} deviates >20%.

Isometric rigor tension changes with ionic strength, as illustrated in Fig. 6. Note that the fibers were put into relaxing solutions of a given ionic strength before incubation in rigor solutions of similar ionic strength. The time constants associated with the recovery between the apparent elastic constants are given in Table 2. The first relaxation time (4 μs) is independent of ionic strength. The second relaxation time (70 μs) is constant within the range of 40 to 160 mM. The variation in this relaxation time in the case of low and high ionic strength solutions is greater than in the other solutions. It cannot be excluded that irreversible changes take place under these ionic

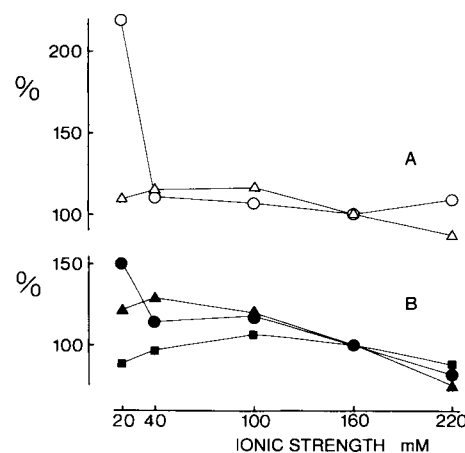


FIGURE 7 Normalized values of the five model parameters of rigor fibers as a function of ionic strength of the incubation solution. (A) μ_2 (open triangles) and μ_3 (open circles). (B) E_1 (solid squares), E_2 (solid triangles), and E_3 (solid circles). All parameter values were normalized to the values obtained under the control conditions (160 mM). Conditions as in Fig. 5.

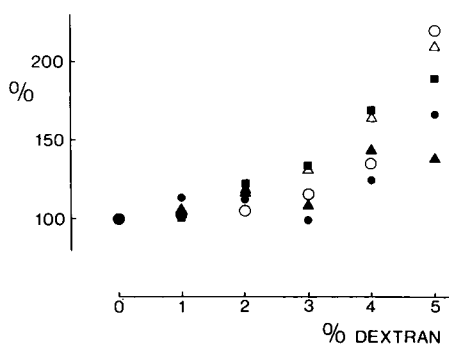


FIGURE 8 Normalized values of the five model parameters of relaxed fibers as a function of Dextran concentration (w/vol). 5% Dextran refers to 50 g of polymer per liter solution. E_1 (solid squares), E_2 (solid triangles); μ_2 (open triangles), E_3 (solid circles), and μ_3 (open circles). All parameter values were normalized to the values at 0% Dextran. Data obtained from eight fibers. Conditions as in Table 4.

strength conditions because control measurements, taken after these incubations, always pointed to loss of isometric tension and changes in fiber stiffness.

The normalized values of the specific model parameters of rigor fibers are given in Fig. 7. In the range of 40 to 160 mM, all parameters were comparable with the values at 160 mM ionic strength. Only the increase of E_3 and μ_3

at 20 mM ionic strength and the decrease of all parameters at 220 mM ionic strength is far more evident than the small variations of the values of the parameters in the range of 40 to 160 mM.

Compressed fibers

The values of the model parameters E_1 , E_2 , E_3 , μ_2 , μ_3 , which were necessary to describe the first 2 ms of the tension transients of compressed relaxed fibers, increase with increasing Dextran concentration (see Fig. 8). The values of the model parameters E_1 and E_2 and μ_2 increase to 130% of the values at control conditions (160 mM ionic strength) in the range of 1 to 3% wt/vol Dextran, whereas in the same range E_3 and μ_3 increase only to 110% of the values at standard conditions.

X-Ray measurements

Typical equatorial x-ray diffraction patterns of activated, rigor, and relaxed fibers are shown in Fig. 9. This figure clearly illustrates the intensity change of the 10 and 11 reflections of relaxed fibers when ionic strength is lowered. The intensity ratio of relaxed fibers at 30 mM is not much different from the ratio of activated fibers at normal ionic strength, although the relaxed fiber does not exert any force. In the case of low ionic strength condi-

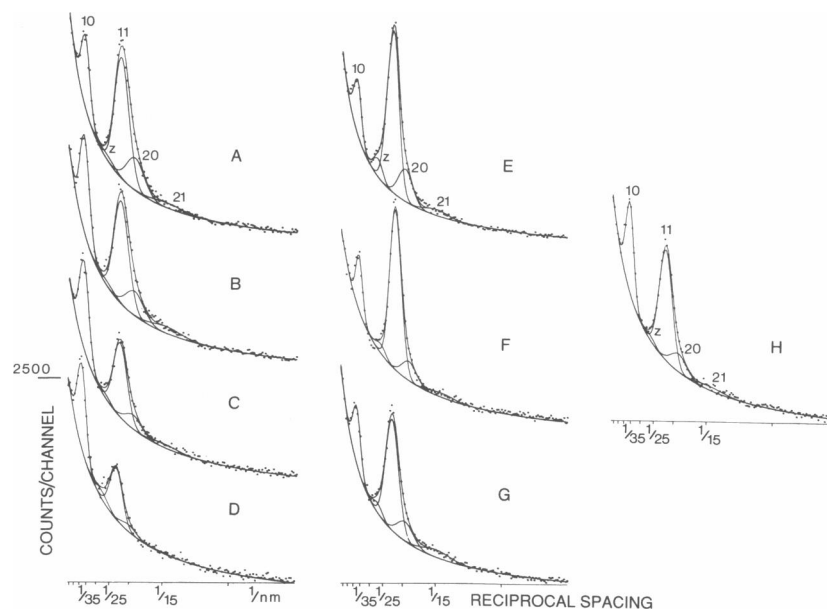


FIGURE 9 Typical equatorial x-ray diffraction patterns of freeze-dried single fibers. In each panel the measured scattering pattern (dots) and the least square fit (solid curve) is shown. The calculated individual peaks (10, 11, 20, 21, and Z-line) are also drawn (solid curves). The measured patterns were corrected for detector characteristics and scattering due to the mica windows of the measuring cells. (A) Pattern obtained from a relaxed fiber, 30 mM ionic strength; (B) relaxed fiber, 50 mM; (C) relaxed fiber, 100 mM; (D) relaxed fiber, 160 mM; (E) pattern obtained from a rigor fiber, 40 mM ionic strength; (F) rigor fiber, 100 mM; (G) rigor fiber, 160 mM (isometric tension 33 kN/m²); (H) pattern obtained from an activated fiber; 160 mM ionic strength (isometric tension 63 kN/m²). Conditions: sarcomere length 2.15 μ m, pH 7.00, temperature 4°C, fiber diameter 150 μ m, fiber length 8.0 mm, experiment 20 September 1986.

tions, high order reflections (20 and 21) are more manifest than under high ionic strength conditions. This could point to less disorder under low ionic strength conditions.

Except for the diffraction pattern at 220 mM, rigor patterns under all ionic strength conditions are similar (see Fig. 9).

The intensity ratio (I_{11}/I_{10}) and the lattice spacing (d_{10}) of rigor and relaxed fibers at various ionic strengths are given in Fig. 10. The lattice spacing of relaxed fibers decreases with decreasing ionic strength (280–50 mM). At 30 mM ionic strength the spacing is comparable with the value at 50 mM.

The lattice spacing in the rigor state does not change between 100 and 160 mM. Lower (20 and 40 mM) as well as higher (220 mM) ionic strength conditions increased the lattice spacing to the values of the relaxed fiber at low ionic strength.

The increment in the intensity ratio of relaxed fibers is rather small in the ionic strength range of 220 to 100 mM, compared with the range of 100 to 30 mM. The intensity ratio of rigor fibers has a maximum value at 100 mM ionic strength. The increment of the I_{11}/I_{10} intensity ratio of relaxed fibers under low ionic strength conditions can be completely attributed to an increased intensity of the I_{11} reflection. The intensity of the I_{10} reflection remains almost unchanged. The A/M ratio of relaxed and rigor fibers at two background levels of the electron density and the total mass above these levels are given in Table 3. It is obvious that the amount of visible mass decreases with increasing ionic strength of the solutions used. This decrease, which points to an increasing disorder in the filament lattice, is far more evident in the case of relaxed fibers than in the case of rigor fibers.

The lattice spacing of relaxed fibers decreases with increasing Dextran concentration. It takes 2–3% wt/vol Dextran to compress the fibers to values of the filament spacing that are comparable with the values of the filament spacing at low ionic strength (30 mM). The intensity ratio I_{11}/I_{10} remains constant within 10%. However, both individual reflections tend to decrease with

TABLE 3 Relative mass (A/M) associated with a thick and thin filament and visible mass as a function of ionic strength

Ionic strength	20	30	40	50	100	160	220
Relaxed state							
A/M low	—	0.304	—	0.239	0.174	0.166	0.120
Mass low	—	1.41	—	1.18	0.98	1.00	0.83
A/M high	—	0.459	—	0.408	0.357	0.354	0.315
Mass high	—	1.26	—	1.11	0.97	1.00	0.87
Rigor state							
A/M low	0.394	—	0.416	—	0.426	0.400	0.330
Mass low	1.08	—	1.06	—	1.02	1.00	0.82
A/M high	0.529	—	0.546	—	0.553	0.528	0.479
Mass high	1.08	—	1.05	—	1.01	1.00	0.86
Activated state							
A/M low	—	—	—	—	—	0.265	—
A/M high	—	—	—	—	—	0.429	—

Relative mass (A/M) associated with the mass ratio of one actin and one myosin filament in the unit cell. The subscripts low and high refer to different positions of the lowest density level. Mass low refers to the total density of the unit cell above the lowest electron density level along the line joining the actin and myosin filaments, whereas mass high refers to the total density of the unit cell above the lowest electron density level in the whole Fourier projection (Haselgrove and Huxley, 1973). Total density of the unit cell at 160 mM is set as 1. Data obtained from five fibers. Conditions as in Fig. 10.

increasing Dextran concentration. Visible mass decreases with increasing Dextran concentration (see Table 4).

DISCUSSION

Comparison of mechanical and x-ray data with data of other studies

Several studies on the stiffness (Brenner et al., 1982, 1986; Schoenberg 1988) and the intensity of the equatorial 11 and 10 reflection (Brenner et al., 1984; Xu et al., 1987) of relaxed fibers or muscles at low ionic strength

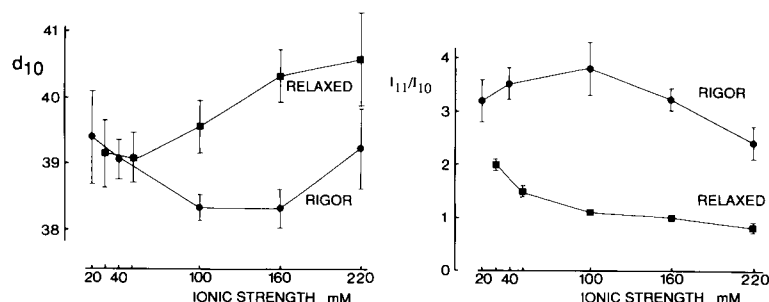


FIGURE 10 Intensity ratio (I_{11}/I_{10}) and lattice spacing (d_{10}) of relaxed and rigor fibers at various ionic strengths of the incubation solutions. Data obtained from five single fibers. Conditions: sarcomere length 2.15 μ m, pH 7.00, temperature 4°C.

TABLE 4 d_{10} , I_{11}/I_{10} , relative mass (A/M) and visible mass as a function of Dextran concentration

Dextran concentration	0%	1%	2%	3%	4%	5%
d_{10}	41.1 ± 0.3	40.7 ± 0.1	39.9 ± 0.4	39.0 ± 0.4	37.5 ± 0.1	37.0
I_{11}/I_{10}	0.90 ± 0.11	0.93 ± 0.13	0.87 ± 0.08	0.89 ± 0.09	1.18 ± 0.08	0.86
A/M low	0.141	0.147	0.136	0.141	0.196	0.136
Mass low	1.00	0.94	0.94	0.85	0.84	0.63
A/M high	0.330	0.333	0.325	0.329	0.369	0.326
Mass high	1.00	0.92	0.94	0.84	0.77	0.65

Intensity ratio (I_{11}/I_{10}), lattice spacing (d_{10}), relative mass (A/M) associated with the mass ratio of one actin and one myosin filament in the unit cell and total density of the unit cell of relaxed fibers incubated in solutions with various concentrations of Dextran (wt/vol). 5% Dextran refers to 50 g of polymer per liter solution. The subscripts low and high refer to different positions of the lowest density level (see Table 3). Total density of the unit cell under control conditions is set as 1. All data, except 5% Dextran (one fiber), obtained from three fibers. Conditions: sarcomere length 2.15 μm , pH 7.00, temperature 4.0 $^{\circ}\text{C}$, ionic strength 160 mM.

have been published. The results were obtained either from frog or rabbit muscle (fibers).

Brenner et al. (1982, 1986) took the slope of the force change vs. length change as apparent stiffness whereas Schoenberg (1988) measured chord stiffness (which is the force generated by a given duration stretch divided by the size of the stretch). They measured an increasing (apparent or chord) stiffness of relaxed fibers when ionic strength of the incubation solution was lowered. This increment of stiffness is dependent on the speed of the length change. The stiffness of relaxed rabbit psoas fibers at low ionic strength (20 mM) was measured by Schoenberg (1988) and Brenner et al. (1986). Schoenberg measured a chord stiffness of $1.17 \times 10^4 \text{ N/m}^2/(\text{nm}/\text{half-sarcomere})$ (speed of stretch $\sim 22,000 \text{ [nm}/\text{half-sarcomere}]/\text{s}$), whereas Brenner measured an apparent stiffness of $2.45 \times 10^4 \text{ N/m}^2/(\text{nm}/\text{half-sarcomere})$ (speed of stretch $\sim 62,000 \text{ [nm}/\text{half-sarcomere}]/\text{s}$). The results differ but it is likely that the observed difference is due to the difference in speed of stretch.

The difference between the stiffness of rigor rabbit psoas fibers measured by Schoenberg ($2.35 \times 10^4 \text{ N/m}^2/[\text{nm}/\text{half-sarcomere}]$; speed of stretch $\sim 2,200 \text{ [nm}/\text{half-sarcomere}]/\text{s}$; 160 mM ionic strength) and Brenner ($2.9 \times 10^4 \text{ N/m}^2/(\text{nm}/\text{half-sarcomere})$; speed of stretch $\sim 10,000 \text{ [nm}/\text{half-sarcomere}]/\text{s}$; 120 mM ionic strength) cannot be due to a difference in the speed of stretch because, as shown by Brenner et al. (1986), rigor stiffness is independent of the speed of stretch (up to stretches with a speed of $10,000 \text{ [nm}/\text{half-sarcomere}]/\text{s}$). The difference could be due to a difference in ionic strength of the rigor solution. However, in frog-muscle fibers we measured only small changes (10%) in the apparent elastic constants of rigor fibers as a function of ionic strength.

Schoenberg has also measured the chord stiffness of rigor frog fibers and relaxed frog fibers at low ionic strength. The chord stiffness of rigor frog fibers ($1.4 \times 10^4 \text{ N/m}^2/[\text{nm}/\text{half-sarcomere}]$) was less than the chord stiffness of rabbit psoas fibers (speed of stretch $\sim 2,200$

$[\text{nm}/\text{half-sarcomere}]/\text{s}$; 160 mM ionic strength). The same can be concluded about the chord stiffness of relaxed frog fibers at low ionic strength ($0.39 \times 10^4 \text{ N/m}^2/[\text{nm}/\text{half-sarcomere}]$) compared with the chord stiffness of relaxed rabbit psoas fibers at low ionic strength (speed of stretch $\sim 22,000 \text{ [nm}/\text{half-sarcomere}]/\text{s}$; 20 mM ionic strength).

The method of measuring stiffness in our experiments differs from the method used by Brenner et al. (1986) and Schoenberg (1988). In our experiments apparent elastic constants and time constants were measured by fitting the tension transients of the fibers, which followed a step-length change, to a model. The five or seven parameters of the model describe the relation between input signal (length change) and output signal (tension response) and are therefore essentially independent of the exact time course of the length change. So, independent of whether we shortened or lengthened the fiber with small ramp-shaped length-changes (1 nm/half-sarcomere, length change completed within 40 μs) or large ramp-shaped length-changes (3 nm/half-sarcomere, length change completed within 40 μs) we always measured the same parameter values at specified conditions.

We measured in relaxed frog-muscle fibers at low ionic strength (30 mM) four apparent elastic constants (E_{app1} , E_{app2} , E_{app3} , and E_{app4}) with the following values: 1.88×10^4 , 0.79×10^4 , 0.23×10^4 , and $0.06 \times 10^4 \text{ N/m}^2/(\text{nm}/\text{half-sarcomere})$. Therefore, we conclude that the apparent stiffness in relaxed rabbit psoas fibers at low ionic strength, as measured by Brenner et al. (1986), is higher than the apparent elastic constants that we measured in relaxed frog fibers at low ionic strength. The chord stiffness value of relaxed frog-muscle fibers, as measured by Schoenberg (1988), is intermediate between the values of the apparent elastic constants E_{app2} and E_{app3} .

We measured in rigor frog-muscle fibers (160 mM) three apparent elastic constants (E_{app1} , E_{app2} , and E_{app3}) with the following values: 4.5×10^4 , 2.24×10^4 , and $1.5 \times$

10^4 N/m²/(nm/half-sarcomere). The stiffness of rigor rabbit psoas fibers as measured by Schoenberg (chord stiffness) and Brenner et al. (apparent stiffness) is higher than the value of the apparent elastic constants E_{app3} that we measure in rigor frog-muscle fibers.

Based on the comparison of the data of rabbit psoas fibers and frog fibers (Schoenberg, 1988) it is concluded that both the chord stiffness of rigor and relaxed fibers at low ionic strength of rabbit fibers is higher than the chord stiffness of the corresponding states of frog fibers.

Based on our stiffness measurements we conclude that at speeds of the length change higher than 10.000 (nm/half-sarcomere)/s stiffness of rigor frog-muscle fibers is speed-dependent because we measured three apparent elastic constants in the tension responses of rigor fibers. The implications of this result, with regard to the estimation of the number of cross-bridges in relaxed fibers (at low ionic strength), will be discussed in the next sections.

Brenner et al. (1984) measured the equatorial diffraction patterns of rigor and relaxed rabbit psoas muscle fibers and Xu et al. (1987) measured these patterns of frog muscles. The intensity of the 10 reflection of relaxed fibers increased to 107% (or 120%) when ionic strength of the incubation solution, in which the rabbit psoas fibers were incubated, was lowered from 170 mM to 20 mM (or 170 mM to 50 mM), whereas the intensity of the 11 reflection increased to 310% (or 248%) (Brenner et al., 1984). In case of relaxed frog muscles the intensity of the 10 reflection increased to 103% and the intensity of the 11 reflection increased to 146% when ionic strength was lowered from 150 mM to 30 mM (Xu et al., 1987). We measured, in case of relaxed single frog-muscle fibers, that the intensity of the 10 reflection increased to 104% and that the intensity of the 11 reflection increased to 203% when ionic strength was lowered from 160 mM to 30 mM. From these results it follows that the changes in the equatorial x-ray data of Brenner et al. (1984), Xu et al. (1987) as well as our data are difficult to interpret in terms of straightforward transfer of mass from the thick filaments to the thin filaments, as discussed by Xu et al. (1987), because the intensity of the 10 reflection does not decrease. Mass shift from the thick filament to the thin filament that occurs when relaxed fibers are incubated in low ionic strength relaxing solutions (relax low μ) can be expressed as a percentage of the mass shift that occurs when fibers are transferred from the normal ionic strength relaxing solution (relax μ) to the normal ionic strength rigor solution (rigor μ). In formula: $[A/M(\text{relax low } \mu) - A/M(\text{relax } \mu)]/[A/M(\text{rigor } \mu) - A/M(\text{relax } \mu)]$.

In case of rabbit psoas fibers this results in a mass-shift of 57% (Brenner et al., 1984). In frog-muscle fibers we measured a similar amount of mass shift (59%). Mass-

shift values of frog muscles calculated in this way are not given by Xu et al. (1987).

Stiffness changes in relaxed fibers

The stiffness of relaxed frog-muscle fibers increases with decreasing ionic strength of the incubation solution. We obtain the following figures if we compare this increased stiffness of relaxed fibers at low ionic strength with the stiffness of rigor fibers. In the case of relaxed fibers of the frog, at 30 mM ionic strength, E_{app1} is close to 45% of E_{app1} of rigor fibers and E_{app2} is 35% of the value of the corresponding parameter in rigor. We obtain a stiffness percentage of 17% and 4% if we compare E_{app3} and E_{app4} of relaxed fibers with E_{app3} of rigor fibers. The question of which of these figures should be taken as a true measure of the number of cross-bridges will be discussed in the last sections of the discussion. However, based on the above mentioned figures, it is concluded that the number of weakly attached cross-bridges in relaxed fibers at low ionic strength relative to the number of attached cross-bridges in rigor will not exceed 45%. This upper limit is obtained by assuming that the immediate stiffness value (E_{app1}) is a true measure of the number of cross-bridges. In the last sections of this discussion we will state that the ionic strength-dependent stiffness increment of E_{app1} (and all the other elastic parameters) is not solely due to an increased number of cross-bridges. Therefore, we can conclude that in relaxed frog-muscle fibers at low ionic strength the number of cross-bridges will be even less than 45%.

The increased stiffness of relaxed muscle fibers at low ionic strength was previously observed in single rabbit psoas fibers (Brenner et al., 1982), whereas Schoenberg (1988) has observed the same phenomena in frog fibers. The measured apparent stiffness of rabbit psoas fibers, at 20 mM ionic strength, depended on the velocity of the length change and reached (much) more than 50% of the rigor apparent stiffness at the fastest stretches possible (Brenner et al., 1986). The measured chord stiffness of frog fibers, at 20 mM ionic strength, depended also on the velocity of the length change and was in the measurements of Schoenberg (1988) ~28% of the rigor chord stiffness at the fastest stretches possible. At first sight the results of our measurements seem to differ from the results of Brenner et al. (1986) because their lower limit equals our upper limit. The recently published results of Schoenberg (1988) indicate that, with regard to this point, the preparations differ. Nevertheless, part of the difference between the results of our measurements and those of Brenner et al. (1986) could be due to differences in the method of comparing the relaxed stiffness with the rigor stiffness.

Brenner et al. (1982, 1986) took the slope of the force change vs. length change as apparent stiffness and Schoenberg (1988) measured chord stiffness. The (apparent or chord) stiffness of relaxed psoas fibers (Brenner et al., 1986; Schoenberg, 1988) and frog fibers (Schoenberg, 1988) at low ionic strength depended on the speed of the length change (speeds up to 22.000 [nm/half-sarcomere]/s, Schoenberg; speeds up to 61.000 [nm/half-sarcomere]/s, Brenner et al.). The (apparent or chord) stiffness of rigor rabbit psoas fibers (Brenner et al., 1986; Schoenberg, 1988) and frog fibers (Schoenberg, 1988) was independent of the speed of the length change (speeds up to 2.200 [nm/half-sarcomere]/s, Schoenberg; speeds up to 10.000 [nm/half-sarcomere]/s, Brenner et al.).

As indicated earlier, we measured apparent elastic constants and time constants, which were independent of the exact time course of the length change, by fitting the tension transients of the fibers, which follow fast step-length changes completed within 40 μ s, to an elastic model. Therefore, we think that we are able to interpret the results of Brenner et al. (1986) and Schoenberg (1988) in terms of the elastic model description used in this paper.

In the case of relatively slow length changes imposed to relaxed fibers at low ionic strength, the processes which correspond to the measured time constants of 4 μ s, 70 μ s, and 1 ms will be completed, which means that only the stiffness that corresponds to E_{app4} will be measured. Using faster length changes, one can measure stiffness that corresponds to E_{app3} . Taking into consideration the duration of the acceleration phase of the length change, we conclude that the length changes with the highest speed (22.000 [nm/half-sarcomere]/s) that were used by Schoenberg (1988) should have enabled him to measure a stiffness between E_{app3} and E_{app2} . With the fastest length changes used by Brenner et al. (1986) (61.000 [nm/half-sarcomere]/s), they should have been able to measure E_{app2} or something intermediate between E_{app2} and E_{app1} , whereas we are able to measure also E_{app1} .

In the case of relatively slow length changes imposed to rigor fibers the processes that correspond to the measured time constants of 4 and 70 μ s will be completed, which means that only the stiffness that corresponds to E_{app3} will be measured. With faster length changes it should be possible to measure E_{app2} or even E_{app1} . Because both Schoenberg (1988) and Brenner et al. (1986) stated that in their experiments rigor stiffness was independent of the speed of the length change it is likely that they measured a (chord or apparent) stiffness of rigor fibers that corresponds to our E_{app3} . This conclusion is supported by the observation that the chord stiffness value of rigor frog fibers as measured by Schoenberg (1988) equals the stiffness value of rigor frog fibers that corresponds with

the E_{app3} value that we measured. Both Brenner et al. and Schoenberg assumed that no higher rigor stiffness would be measured with speeds of stretch higher than they used. Therefore, it seemed reasonable to compare rigor stiffness measured with a medium speed of the length change (2.200 [nm/half-sarcomere]/s, Schoenberg or 10.000 [nm/half-sarcomere]/s, Brenner et al.) with the apparent stiffness of relaxed fibers measured with speeds up to 22.000 [nm/half-sarcomere]/s (Schoenberg, 1988) or 61.000 [nm/half-sarcomere]/s (Brenner et al., 1986). However, we measured a speed-dependent rigor stiffness in frog fibers which makes it likely that their assumption was wrong.

We conclude, taking the foregoing into consideration, that to obtain a correct comparison between the stiffness of relaxed fibers and the stiffness of rigor fibers one should stretch fibers in both states with the same velocity or one should compare the values of similar apparent elastic constants. As mentioned above the latter procedure results in a stiffness of relaxed frog-muscle fibers at low ionic strength that does not exceed 45% of the stiffness of rigor fibers. Brenner et al. (1986) may have overestimated the number of cross-bridges in relaxed rabbit psoas fibers at low ionic strength as indicated above, although it is also likely that the apparent stiffness of relaxed rabbit psoas fibers relative to the stiffness of rigor rabbit psoas fibers is higher than in the case of frog fibers (Schoenberg, 1988).

Changes in equatorial diffraction patterns of relaxed fibers

Two significant changes can be seen in the equatorial diffraction patterns obtained from relaxed fibers incubated in solutions of various ionic strength. The filament spacing decreases with decreasing ionic strength (in the range 220 to 50 mM). Such an effect has been seen earlier in the range of 300 to 20 mM in several species (Brenner et al., 1984; Matsubara et al., 1985; Umazume et al., 1986). The effect of increasing intensity ratio I_{11}/I_{10} with decreasing ionic strength has been observed in single rabbit psoas fibers (Brenner et al., 1984) and recently in frog muscle (Xu et al., 1987). The increment of this intensity ratio at low ionic strength relative to the ratio of relaxed fibers at normal ionic strength as measured in our single frog fibers (2.00) is closer to the results of Brenner et al. (1984) (2.22) than to the results of Xu et al. (1987) (1.33). However, a direct comparison between the results is not possible, because effects due to disorder, which occur with increasing ionic strength, can be dependent on the species or preparations (Brenner et al., 1984; Matsubara et al., 1985; Matsuda and Podolsky, 1984). It follows from this ordering effect under low ionic strength condi-

tions, that mass shift values as given in Table 3 cannot be interpreted unambiguously in terms of numbers of attached cross-bridges. However, the changes in the A/M ratio of relaxed fibers at low ionic strength relative to the changes in the A/M ratio between relaxed fibers and rigor fibers could indicate that 59% of the number of cross-bridges of rigor fibers are present in relaxed fibers at low ionic strength. Results of Brenner et al. (1984) indicate that in rabbit psoas fibers 57% of the number of rigor cross-bridges could be present in the relaxed fibers at low ionic strength. Although Xu et al. (1987) did not give A/M ratio figures, it follows from their results that the number of weakly attached cross-bridges in relaxed frog muscle at low ionic strength relative to the number of attached cross-bridges in rigor will be less than the above-mentioned figures. Two obvious differences between the experimental conditions at which the results of our measurements and those of Xu et al. (1987) were obtained could perhaps be correlated with the differences in mass shift. First, we used skinned single fibers of the frog. Within few (<3) minutes of incubation in the appropriate solution the rigor state, the activated state, or the low-ionic-strength relaxed state could be induced in these fibers. Xu et al. (1987) used skinned muscle of the frog. They stated that it took 20–40 min to exchange the relaxing solution in the muscle by the rigor solution. Furthermore, they compressed the normal as well as the low-ionic-strength frog sartorius muscle by adding 2% PVP-40 to the incubation solutions. We showed that fibers could be easily compressed without changing the intensity ratio I_{11}/I_{10} at 160 mM ionic strength. However, it remains unclear how the intensity ratios at low ionic strength are influenced by the addition of PVP-40. In relation to this, Xu et al. (1987) found a larger filament spacing at low ionic strength compared with normal ionic strength with PVP added in both solutions.

Stiffness and diffraction pattern changes in rigor fibers

Rigor fibers have elastic constants clearly different from those of relaxed fibers at all ionic strengths. The same applies to the equatorial diffraction pattern. Isometric tension exerted by the fiber increases twice in the ionic strength range of 220 to 20 mM, although d_{10} , the intensity ratio I_{11}/I_{10} and the apparent elastic constants change only slightly. Two effects could be responsible for this observed result. The tension increment in the range of 160 to 20 mM could be the result of an increased d_{10} distance. Variation in filament spacing induced by pH or Dextran-500 leads to a tension increment (Podolsky et al., 1982). The decrement of the A/M mass ratio in the range of 100 to 220 mM could point to a decreased number of

rigor cross-bridges under high ionic strength conditions and thus to a tension decrement. Under high ionic strength conditions (220 mM) disordering effects are observed. This could, together with an increased value of d_{10} (also observed by Matsubara et al., 1985), support the idea that a decreased amount of cross-bridges is present at high ionic strength. It is likely that the magnitude of the apparent elastic constants of rigor fibers, as a function of the ionic strength of the incubation solutions, is correlated with the filament spacing and the mass associated with the actin filament (which should be an indication of the number of cross-bridges). The observed changes in the apparent stiffness are small, especially in the ionic strength range of 50 to 120 mM (<10%). This is comparable with the observation of Tawada and Kimura (1984) that rigor stiffness in psoas fibers does not change with changes in ionic strength.

Origin of model parameters

The model independent description of the measured tension responses consists of apparent elastic constants (E_{app}) and time constants (τ_i). The apparent elastic constants changed with the filament spacing and the mass associated with the actin filament, in rigor as well as in relaxed fibers. The two fastest time constants (4 and 70 μ s) of relaxed and rigor fibers did not change with changes in ionic strength of the solutions. The slower time constant (1 ms), which becomes visible in relaxed fibers under low-ionic-strength conditions, is absent or very small under normal ionic strength conditions. In a previous paper (Jung et al., 1988b) we argued that these fastest time constants, which appeared to be present in the relaxed state as well as in the rigor and Ca^{2+} -activated state, cannot be the result of viscous drag between the filaments only. The results from stiffness measurements at various ionic strengths support this view. If the observed time constants are caused only by drag dependent on filament spacing, one expects equal model damping coefficients in the case of fibers with equal filament spacing, even in different states (e.g., rigor, relaxation, or activation). This is not the case. At comparable filament spacing, a discrepancy between the coefficients is still present, although the damping coefficients μ_2 and μ_3 of relaxed fibers do increase with decreasing ionic strength (and decreasing filament spacing) (see Fig. 4) and the damping coefficients of rigor fibers remain fairly constant. The values of damping coefficient μ_2 and μ_3 are 80 and 250 Ns/m² (at 160 mM); 140 and 680 Ns/m² (at 30 mM) in the case of relaxed fibers, and 330 and 6,000 Ns/m² in the case of rigor fibers. The values of the damping coefficient μ_2 and μ_3 in compressed fibers, with a filament spacing comparable to relaxed fibers at low ionic

strength, are 105 and 275 Ns/m² (3% wt/vol Dextran). It follows from these values that μ_2 is influenced by filament spacing changes, which could point to effects due to viscous drag, as well as by mass transfer. The influence of the filament spacing on the value of μ_3 is small. Mass transfer (number of cross-bridges) has a greater influence on this parameter. In summary, the model parameters μ_2 and μ_3 , which represent damping coefficients and which imply two fast recoveries, are for a part, certainly in the case of relaxed fibers at 160 mM ionic strength, caused by passive structures or viscous drag. An appreciable part of the magnitude of these two constants is caused by the presence of mass between the filaments, either as attached cross-bridges, in the case of rigor fibers, or weakly attached cross-bridges, in the case of relaxed fibers at low ionic strength.

Stiffness of weakly attached cross-bridges

We see, while lowering the ionic strength of the incubation solution, three effects in the case of relaxed fibers: an increasing stiffness, a decreasing filament spacing, and a mass shift towards the actin filament. All three effects are correlated with each other. Brenner et al. (1982, 1984) also reported an increment of stiffness of psoas fibers, while the filament spacing decreased and the intensity ratio I_{11}/I_{10} increased at low ionic strength. It remained unclear how both effects contributed to the stiffness. In the case of relaxed fibers, the addition of various concentrations of PVP (Umazume et al., 1986; Matsubara et al., 1984) or Dextran (Matsubara et al., 1985; Brenner et al., 1984) leads to a decreased filament spacing and an increased stiffness (Goldman and Simmons, 1986). At least a part of the stiffness increment under low ionic strength conditions can be attributed to a decreased filament spacing.

Stiffness measurements and equatorial x-ray diffraction patterns of relaxed fibers incubated in solutions with various Dextran concentrations showed that the stiffness increment, expressed in E_1 , E_2 , and E_3 , is correlated with the decrement of filament spacing (see Fig. 8 and Table 4), whereas the intensity ratio did not change with filament spacing. The values of the parameters E_1 and E_2 , at a filament spacing comparable with the spacing under low ionic strength conditions (2–3% Dextran), increased to 130% of the stiffness under control (160 mM) conditions, whereas E_3 increased only to 110%. This means that a major part of the observed parameter increment in the ionic strength range of 220 to 100 mM can be attributed to the decrement in filament spacing (see Fig. 4). The filament spacing under low-ionic-strength conditions (30 and 50 mM) remains almost constant, whereas the incre-

ment of stiffness and the shift of mass becomes more obvious. The value of the model parameter E_1 at 30 mM ionic strength is ~175% of the value at normal ionic strength (160 mM), whereas E_2 and E_3 increase to 300% of the values at normal ionic strength. It is obvious that under these low ionic strength conditions the contribution of increased mass near the actin filament to the increment of E_2 and E_3 exceeds the contribution due to filament spacing changes. These results suggest that the elastic element E_3 is influenced most by mass transfer and hardly by filament spacing changes, whereas the elastic parameter E_1 is influenced by filament spacing and mass shift in equal amounts. This observation limits the conclusions drawn from the immediate stiffness measurements. If we compare E_1 (equals E_{appl}) of low ionic strength relaxed fibers with E_1 of rigor fibers, bearing in mind that half of the increment of E_1 is due to changes in filament spacing, and we still assume that this immediate stiffness is a measure of number of attached cross-bridges, then we can conclude that in case of relaxed frog muscle fibers ~30% of the number of rigor cross-bridges is present at low ionic strength (30 mM). However, in a previous article (Jung et al., 1988b) we concluded that E_{appl} is probably not a true measure of numbers of attached cross-bridges. Which leaves us only E_{app2} (and E_2) and E_{app3} (and E_3) as a measure of cross-bridges. The major changes of E_2 (and E_{app2}) are induced by the mass shift at low ionic strength, although this parameter is also influenced by filament spacing changes induced by Dextran. If we assume that rigor and relaxed fibers have cross-bridges with the same intrinsic cross-bridge stiffness and E_2 (or E_{app2}) is a measure of the number of cross-bridges, than the number of attached cross-bridges in relaxed fibers would be 30% of the number of cross-bridges attached in rigor fibers. However, Jung et al. (1988b) argued that with respect to the comparison of stiffness of rigor and activated fibers E_{app3} or E_3 are probably better measures of number of cross-bridges than E_{app2} or E_2 . We show in this paper that E_3 , just as E_{app3} , did not change much with filament spacing, which supports this statement. If we take these parameters as a measure of the number of cross-bridges in the rigor state as well as in the relaxed state at low ionic strength we obtain a percentage of about 17% (in case of E_{app3}) or 9% (in case of E_3). In summary, if we assume that weakly attached cross-bridges have similar intrinsic cross-bridge stiffness as rigor cross-bridges than the elasticity measurements lead to the conclusion that 10–30% of the number of rigor cross-bridges are present in relaxed fibers at 30 mM ionic strength. EPR measurements revealed that a similar percentage of myosin heads under low ionic strength relaxing conditions is oriented at the same angle as in rigor, but with more disorder (Fajer et al., 1985).

There is no depletion of MgATP, and the two-

dimensional x-ray diffraction patterns show that the myosin and actin based layer line patterns of relaxed fibers at low ionic strength differ from those of rigor fibers (Matsuda and Podolsky, 1984; Xu et al., 1987). This means that the observed mass shift and the increased stiffness of relaxed fibers at low ionic strength are not the result of a small number of rigor cross-bridges. The occurrence of a 1-ms time constant, which is absent in rigor fibers under all ionic strength conditions, supports this view. The 1-ms time constant, which is probably associated with weakly attached cross-bridges, could point to a rapid detachment of these cross-bridges. The relaxed fibers exerted no force at low ionic strength, which excludes the occurrence of force generating cross-bridges.

Xu et al. (1987) and Brenner et al. (1984) pointed to the difficulties in interpreting the intensity changes, due to disorder effects. Nevertheless, Brenner et al. (1984) concluded that a significant number of cross-bridges are present at low ionic strength in relaxed psoas fibers. They concluded that probably the attachment of these cross-bridges is different from the attachment of rigor cross-bridges. Xu et al. (1987) concluded that the mass transfer, which would be due to attached cross-bridges with a not sharply defined orientation relative to actin, will be substantially less than the I_{11} intensity change of 46% that they observed. The intensity changes in our preparation were closer to the values obtained by Brenner et al. (1984) (single rabbit psoas fibers) than those mentioned by Xu et al. (1987) which were obtained from frog fiber bundles. At least 50% of the number of rigor cross-bridges would be present in relaxed fibers (30 mM) if we just take the A/M ratio as a measure of cross-bridges.

In summary, if the cross-bridges stiffness of weakly attached cross-bridges is comparable with the cross-bridge stiffness of rigor cross-bridges (as follows from the mechanical results), then it is concluded that the number of attached cross-bridges in relaxed fibers at low ionic strength is less than one would expect from the x-ray data. On the other hand, there could be a large number of attached cross-bridges in relaxed fibers at low ionic strength (as could follow from the x-ray results) but then the intrinsic cross-bridge stiffness of these weakly attached cross-bridges has to be 0.5–0.75 (with respect to E_1 , E_2 , or E_{app2}) or, which is more likely, 0.16 (with respect to E_3 or E_{app3}) of the stiffness of rigor cross-bridges. Independent of these two possibilities we can conclude that the number of weakly attached cross-bridges in relaxed frog muscle fibers at control conditions (160 mM) will be negligible (<5%), because both methods indicate that the major changes in stiffness or mass shift, which could point to weakly attached cross-bridges, only take place at extremely low ionic strength conditions (30–50 mM).

Weakly attached cross-bridges in activated fibers

It follows from the above mentioned arguments that it remains difficult to estimate the number of attached cross-bridges present in the activated state. The equatorial diffraction patterns of relaxed fibers at low ionic strength and activated fibers (160 mM) are comparable. This could mean that in both states comparable numbers of cross-bridges are present. One could argue that either a significant number of weakly attached cross-bridges is present in activated fibers or that the number of weakly attached cross-bridges in activated fibers is negligible. The first possibility is not very attractive because one has to assume that the intrinsic stiffness and force of the force generating cross-bridges is much higher than the intrinsic stiffness and force of the rigor cross-bridges (see also Jung et al., 1988b). Furthermore, a large number of weakly attached cross-bridges in activated fibers suggest that stiffness measurements cannot be used as a measure of the number of cross-bridges in case of activated and rigor fibers. Thus the latter possibility seems to be more likely.

In summary, equatorial x-ray diffraction patterns and stiffness measurements with microsecond time resolution point to the existence of weakly attached cross-bridges in frog muscle fibers at low ionic strength. We have argued that the number of these cross-bridges at low ionic strength will be small, although an exact estimate of the number of these cross-bridges cannot be given. It is likely that the stiffness contribution of weakly attached cross-bridges to the stiffness of the activated fiber or the relaxed fiber under normal ionic strength conditions will be limited to a negligible magnitude.

We thank Dr. H. Gerritsen (Synchrotron Radiation Source, Daresbury, UK) for assistance during the x-ray measurements, Mr. R. Schuurhof, Mr. A. A. Meijer, Mr. J. Volkerling, and Mr. R. J. Bakker for technical assistance.

This study was supported by the Netherlands Organization for the Advancement of Pure Research (ZWO), also in connection with the agreement between the Science and Engineering Research Council and ZWO concerning the Synchrotron Radiation Source.

Received for publication 17 October 1988 and in final form 17 November 1988.

REFERENCES

- Blangé, T., and G. J. M. Stienen. 1985a. The early part of the tension transient of activated skinned muscle fibres of the frog at high time resolution. *J. Physiol. (Lond.)* 366:74P.
- Blangé, T., and G. J. M. Stienen. 1985b. Transmission phenomena and early tension recovery on skinned muscle fibres of the frog. *Pfluegers Arch. Eur. J. Physiol.* 405:12–18.

- Blangé, T., D. W. G. Jung, G. J. M. Stienen, and B. W. Treijtel. 1987. Comparison of fast recovery in activated and rigor skinned frog muscle fibres. *J. Muscle Res. Cell Motil.* 8:65.
- Brenner, B., M. Schoenberg, J. M. Chalovich, L. E. Greene, and E. Eisenberg. 1982. Evidence for cross-bridge attachment in relaxed muscle at low ionic strength. *Proc. Natl. Acad. Sci. USA.* 79:7288–7291.
- Brenner, B., L. C. Yu, and R. J. Podolsky. 1984. X-Ray diffraction evidence for cross-bridge formation in relaxed muscle fibres at various ionic strengths. *Biophys. J.* 46:299–306.
- Brenner, B., J. M. Chalovich, L. E. Greene, E. Eisenberg, and M. Schoenberg. 1986. Stiffness of skinned rabbit psoas fibers in MgATP and MgPP_i solution. *Biophys. J.* 50:685–691.
- Fabiato, A., and F. Fabiato. 1979. Calculator programs for computing the composition of the solutions containing multiple metals and ligands used for the experiments in skinned muscle cells. *J. Physiol. (Paris)*. 75:463–505.
- Fajer, P., E. Fajer, E. Svensson, N. Brunsvold, C. Wendt, and D. D. Thomas. 1985. EPR studies of muscle contraction at low ionic strength. *Biophys. J.* 47:380a.
- Ford, L. E., A. F. Huxley, and R. M. Simmons. 1977. Tension responses to sudden length change in stimulated frog muscle fibres. *J. Physiol. (Lond.)*. 269:441–515.
- Godt, R. E., and B. D. Lindley. 1982. Influence of temperature upon contractile activation and isometric force production in mechanically skinned muscle fibres of the frog. *J. Gen. Physiol.* 80:279–297.
- Goldman, Y. E., and R. M. Simmons. 1986. The stiffness of frog skinned muscle fibres at altered lateral filament spacing. *J. Physiol. (Lond.)*. 378:175–194.
- Haselgrove, J. C., and H. E. Huxley. 1973. X-Ray evidence for radial cross-bridge movement and the sliding filament model in actively contracting skeletal muscle. *J. Mol. Biol.* 77:549–568.
- Jung, D. W. G., T. Blangé, H. de Graaf, and B. W. Treijtel. 1987. Evidence for weakly attached cross-bridges in skinned frog muscle fibres. *J. Muscle Res. Cell Motil.* 8:63–64.
- Jung, D. W. G., T. Blangé, H. de Graaf, and B. W. Treijtel. 1988a. The stiffness of weakly attached cross-bridges in relaxed frog muscle fibres. *Biophys. J.* 53:567a.
- Jung, D. W. G., T. Blangé, H. de Graaf, and B. W. Treijtel. 1988b. Elastic properties of relaxed, activated and rigor muscle fibers measured with microsecond resolution. *Biophys. J.* 54:897–908.
- Matsubara, I., Y. E. Goldman, and R. M. Simmons. 1984. Changes in the lateral filament spacing of skinned muscle fibres when cross-bridges attach. *J. Mol. Biol.* 173:15–33.
- Matsubara, I., Y. Umazume, and N. Yagi. 1985. Lateral filamentary spacing in chemically skinned murine muscles during contraction. *J. Physiol. (Lond.)*. 360:135–148.
- Matsuda, T., and R. J. Podolsky. 1984. X-Ray evidence for two structural states of the actomyosin cross-bridge in muscle fibers. *Proc. Natl. Acad. Sci. USA.* 81:2364–2368.
- Moiescu, D. G., and R. Thieleczek. 1978. Calcium and strontium concentration changes within skinned muscle preparations following a change in external bathing solution. *J. Physiol. (Lond.)*. 275:241–262.
- Podolsky, R. J., G. R. S. Naylor, and T. Arata. 1982. Cross-bridge properties in the rigor state. In *Basic Biology of Muscles: A Comparative Approach*. B. M. Twarog, R. J. C. Levine, and M. M. Dewey, editors. Raven Press, New York. 79–89.
- Schoenberg, M. 1988. Characterization of the myosin adenosine triphosphate (M.ATP) crossbridge in rabbit and frog skeletal muscle fibers. *Biophys. J.* 54:135–148.
- Stienen, G. J. M., and T. Blangé. 1985. Tension responses to rapid length changes in skinned muscle fibres of the frog. *Pfluegers Arch. Eur. J. Physiol.* 405:19–23.
- Stienen, G. J. M., K. Güth, and J. C. Rüegg. 1983. Force and force transients in skeletal muscle fibres of the frog skinned by freeze-drying. *Pfluegers Arch. Eur. J. Physiol.* 397:272–276.
- Tawada, K., and M. Kimura. 1984. Stiffness of glycerinated rabbit psoas fibers in the rigor state. *Biophys. J.* 45:593–602.
- Umazume, Y., S. Onodera, and H. Higuchi. 1986. Width and lattice spacing in radially compressed frog skinned muscle fibres at various pH values, magnesium ion concentrations and ionic strengths. *J. Muscle Res. Cell Motil.* 7:251–258.
- van den Hooft, H., T. Blangé, and L. H. van der Tweel. 1982. A displacement servosystem for muscle research permitting 50 μ m length changes within 40 μ s. *Pfluegers Arch. Eur. J. Physiol.* 395:152–155.
- Xu, S., M. Kress, and H. E. Huxley. 1987. X-Ray diffraction studies of the structural state of cross-bridges in skinned frog sartorius muscle at low ionic strength. *J. Muscle Res. Cell Motil.* 8:39–54.